

# RSC Advances



This is an *Accepted Manuscript*, which has been through the Royal Society of Chemistry peer review process and has been accepted for publication.

*Accepted Manuscripts* are published online shortly after acceptance, before technical editing, formatting and proof reading. Using this free service, authors can make their results available to the community, in citable form, before we publish the edited article. This *Accepted Manuscript* will be replaced by the edited, formatted and paginated article as soon as this is available.

You can find more information about *Accepted Manuscripts* in the [Information for Authors](#).

Please note that technical editing may introduce minor changes to the text and/or graphics, which may alter content. The journal's standard [Terms & Conditions](#) and the [Ethical guidelines](#) still apply. In no event shall the Royal Society of Chemistry be held responsible for any errors or omissions in this *Accepted Manuscript* or any consequences arising from the use of any information it contains.

Cite this: DOI: 10.1039/c0xx00000x

www.rsc.org/xxxxxx

ARTICLE TYPE

## Effect of riboflavin concentration on the development of photo-cross-linked amniotic membranes for cultivation of limbal epithelial cells

Jui-Yang Lai,\*<sup>a</sup> and Li-Jyuan Luo<sup>a</sup>*Received (in XXX, XXX) Xth XXXXXXXXX 20XX, Accepted Xth XXXXXXXXX 20XX*

DOI: 10.1039/b000000x

To overcome the limitations of low stability of tissue collagens and possible toxicity of chemical cross-linkers, the amniotic membrane (AM) was photo-cross-linked by ultraviolet (UV) irradiation in the presence of riboflavin. This study aims to investigate the effect of photoinitiator concentration on the preparation of photo-cross-linked AM materials for cultivation of limbal epithelial cells (LECs). The number of cross-links per unit mass of collagen matrix was significantly increased with increasing riboflavin concentration from 0.1 to 10 mg/ml. In addition, the equilibrium water content, ultrastructure, nanotopography, and enzymatic degradability of AM samples were found to be associated with the cross-linked structure of UV-irradiated biological tissues. Human corneal epithelial cellular responses to photo-cross-linked AM were assessed by measuring the mitochondrial dehydrogenase activity and interleukin-6 expression levels. Irrespective of the riboflavin concentration, the test samples were fully biocompatible and retained anti-inflammatory activities, probably due to the absence of exogenous cross-linker molecules in the proteinaceous matrices following cross-linking reaction. Results of quantitative real-time reverse transcription polymerase chain reaction and Western blot analyses showed that the LECs cultured on the AM substrates with different cross-linking densities had varying levels of enhanced stemness. The expressions of ABCG2 at mRNA and protein levels were significantly up-regulated with increasing surface roughness of physically cross-linked biological tissue materials. For the first time, here we report that the riboflavin concentration may play an important role in the modulation of properties of photo-cross-linked AM as a new LEC carrier.

### Introduction

The amniotic membrane (AM) is the innermost layer of the placenta that is featured with low immunogenicity, anti-inflammatory, anti-angiogenic, and anti-scarring properties.<sup>1</sup> In the research field of tissue engineering, the AM-based strategy has been applied for the reconstruction of bladder defects<sup>2</sup> and the treatment of skin wounds.<sup>3</sup> Investigators have also reported that this biological tissue material can be used as a carrier for ex vivo expanded corneal epithelial stem cells as bioengineered ocular surface.<sup>4</sup> Transplantation of autologous limbal epithelial cells (LECs) cultivated on AM matrices is demonstrated as an effective technique for the restoration of vision in patients with unilateral limbal stem cell deficiency.<sup>5</sup> Although the AM has been clinically shown to help management of ocular surface diseases, such as thermal or chemical burns, corneal ulcers, ocular cicatricial pemphigoid, and Stevens-Johnson's syndrome, the matrix material itself appears to be limited by rapid degradation and resorption in vivo.<sup>6</sup> When used in certain corneal disorders causing increased action of tissue collagenase,<sup>7</sup> the AM transplants may experience an accelerated disintegration.

It is known that the collagen molecules constitute a major portion of human AM tissues.<sup>8</sup> In order to improve the stability of

tissue collagen, the AM has been chemically modified by means of exogenous agents. In our laboratory, the cross-linkers belong to either zero-length (i.e., carbodiimide)<sup>9</sup> or non-zero-length (i.e., glutaraldehyde)<sup>10</sup> are recently used to reinforce the structural strength of AM materials. However, it has been documented that the possibility of inducing cytotoxicity cannot be excluded during the treatment of biomaterials with chemical cross-linkers. When cross-linked with glutaraldehyde, the biopolymers including hyaluronic acid,<sup>11</sup> chitosan,<sup>12</sup> and gelatin<sup>13</sup> typically show very poor biocompatibility with ocular cells, probably due to the specific linkages present in the cross-linking structure. On the other hand, water-soluble carbodiimides are considered as safe alternatives of cross-linkers because they can induce cross-link formation without taking part in the linkages.<sup>14</sup> Although the resultant by-products of the cross-linking reaction are in the form of urea derivatives, it is noteworthy that carbodiimide over certain concentrations may also pose a risk of significant harm to the cultured cells.<sup>15</sup>

Actually, corneal cross-linking is a commonly used clinical procedure for the stabilization of tissue collagen by strengthening the chemical bonds of biological materials. Riboflavin in combination with ultraviolet (UV) light has proven to be effective in preventing disease progression in patients with keratoconus.<sup>16</sup> By means of UV irradiation technique, we have made an attempt

to sterilize the thermo-responsive poly(*N*-isopropylacrylamide)-grafted culture support, which is beneficial to fabricate transplantable corneal endothelial cell sheets for tissue reconstruction.<sup>17</sup> On the other hand, given that the UV irradiation presents the inherent ease of implementation and merits with respect to safety and cost, the copolymers composed of poly(2-hydroxyethyl methacrylate) and poly(acrylic acid) are successfully synthesized by us via UV-initiated free radical polymerization.<sup>18</sup> As potential keratoprosthetic biomaterials, the copolymer hydrogels are further designed by changing the processing parameter such as concentration of photoinitiator (i.e., 2,2-diethoxyacetophenone).

In view of these earlier observations, this study was undertaken to develop photo-cross-linked AM materials for application to the cultivation of LECs. The influence of photoinitiator concentration on the properties of UV-irradiated biological tissues was investigated. Before exposure to UV for the duration of 20 min, the AM samples were pretreated with different concentrations of riboflavin. The initiating free radicals were generated when illuminated with UV light. Then, the cross-linking density and water content measurements were performed to characterize the cross-linked structure of AM and to estimate its water absorbing capacity. The photo-cross-linking-mediated alterations in AM ultrastructure and nanotopography were confirmed by transmission electron and atomic force microscopy studies. The enzymatic degradability of AM tissues treated with riboflavin and UV light was determined to evaluate the matrix stability. The *in vitro* biocompatibility of photo-cross-linked AM materials was assessed by measuring the viability of human corneal epithelial cells. The cellular response was also monitored, analyzing the anti-inflammatory activity of test samples. After cultivation of LECs on AM substrates, quantitative real-time reverse transcription polymerase chain reaction and Western blot analyses were conducted to further explore cell stemness associations with cross-linking density and surface roughness of biological materials.

## Experimental

### Materials

This study followed the tenets of the Declaration of Helsinki involving human subjects and received approval from the Institutional Review Board of our institution. Human AM tissues (i.e., the innermost layer of the placental membranes) were obtained with informed consent at the time of elective cesarean section from mothers when human immunodeficiency virus, syphilis, and hepatitis B and C had been excluded by serologic tests. The separation of AM was carried out using blunt dissection to cut the tissue samples approximately 2 cm from the placental disc. The average thickness of AM samples used in this work was 100  $\mu\text{m}$ . Riboflavin-5-monophosphate, dextran, collagenase (type I *Clostridium histolyticum*, EC 3.4.24.3), and lipopolysaccharide (LPS) were purchased from Sigma-Aldrich (St. Louis, MO, USA). Dimethyl sulfoxide (DMSO) was obtained from J.T.Baker (Phillipsburg, NJ, USA). Deionized water used was purified with a Milli-Q system (Millipore, Bedford, MA, USA). Phosphate-buffered saline (PBS, pH 7.4) was purchased from Biochrom (Berlin, Germany). Balanced salt solution (BSS,

pH 7.4) was obtained from Alcon Laboratories (Fort Worth, TX, USA). Dispase II was purchased from Roche Diagnostics (Indianapolis, IN, USA). FNC Coating Mix (i.e., a fibronectin/collagen mixture) was obtained from Athena ES (Baltimore, MD, USA). Dulbecco's modified Eagle's medium (DMEM), keratinocyte serum-free medium (KSFM), Ham's F-12 nutrient mixture (Ham's F-12), gentamicin, trypsin-ethylenediaminetetraacetic acid (EDTA), and TRIzol reagent were purchased from Gibco-BRL (Grand Island, NY, USA). Fetal bovine serum (FBS) and the antibiotic/antimycotic (A/A) solution (10,000 U/ml penicillin, 10 mg/ml streptomycin and 25  $\mu\text{g}/\text{ml}$  amphotericin B) were obtained from Biological Industries (Kibbutz Beit Haemek, Israel). 24-well tissue culture polystyrene (TCPS) plates (Falcon 353047) were purchased from Becton Dickinson Labware (Franklin Lakes, NJ, USA). All the other chemicals were of reagent grade and used as received without further purification.

### Preparation of photo-cross-linked amniotic membranes

The AM samples were aseptically washed three times with PBS containing 1% A/A solution and 50  $\mu\text{g}/\text{ml}$  of gentamicin according to the protocols reported previously.<sup>10</sup> The membranes were immersed with sequential concentrations of DMSO, followed by freezing and storing at  $-80^\circ\text{C}$  in DMEM containing 50% glycerol. After a further incubation with 0.02% EDTA at  $37^\circ\text{C}$ , the AM was denuded of its amniotic epithelial cells by gentle scraping. For photo-cross-linking of biological tissues, the riboflavin-5-monophosphate was dissolved in PBS containing 20% dextran to concentrations of 0.1, 1, and 10 mg/ml. Then, the riboflavin-treated AM materials were subjected to irradiation using the Blak-Ray high intensity UV lamp (UVP, Upland, CA, USA) with 365 nm. Samples were placed at a distance of 25 cm from the radiation source and exposed to UV irradiation with a light intensity of 5  $\text{mW}/\text{cm}^2$  for 20 min. In this study, the AM matrices treated with different concentrations of riboflavin were respectively designated as AM-0.1, AM-1, and AM-10. The biological tissues without photo-cross-linking (AM-0) were used for comparison.

### Cross-linking density measurements

The cross-linked structure of the UV-irradiated AM such as degree of cross-link and average molecular weight of polymer chains between two consecutive junctions was analyzed according to the method reported previously.<sup>19</sup> After immersion in deionized water for 12 h at  $25^\circ\text{C}$ , the photo-cross-linked membranes (20 mm  $\times$  10 mm) were mounted between two clamps of an Instron Mini 44 universal testing machine (Canton, MA, USA). The lower clamp was then adjusted downward until the sample was just in tension and the unstressed length was noted. Following determination of mechanical properties, the test specimens were removed from the clamps and blotted with tissue paper, and the density was determined by the specific gravity bottle method. A graph of  $\sigma$  against  $(\alpha - \alpha^2)$  would be a straight line with the slope giving  $RT\rho V^{1/3}/M_c$ , where  $\sigma$  = the force per unit area of the swollen unstretched sample;  $\alpha$  = extension ratio;  $R$  = gas constant;  $T$  = absolute temperature;  $\rho$  = density of sample;  $V$  = volume fraction; and  $M_c$  = average molecular weight of the chains between cross-links. The number of cross-links per unit mass would be given by  $(2M_c)^{-1}$ . Results were the average of

four independent measurements.

#### Water content measurements

For water content measurements, the AM samples were first dried to constant weight ( $W_i$ ) in vacuo and were immersed in deionized water at 37°C with reciprocal shaking (50 rpm) in a thermostatically controlled water bath. After 6 h, the swollen membranes weighed ( $W_s$ ), and the equilibrium water content (%) of the test sample was defined by  $((W_s - W_i)/W_s) \times 100$ . Results were averaged on four independent runs.

#### Transmission electron microscopy

Specimens were processed for transmission electron microscopy (TEM) studies as described previously.<sup>10</sup> Various preparations of AM were fixed with 2% glutaraldehyde in 0.1 M cacodylic acid buffer (pH 7.4) overnight at 4°C. After rinsing them with 0.1 M cacodylic acid buffer, the samples were post-fixed in 1% osmium tetroxide and dehydrated in a graded series of ethanol solutions. The tissue specimens were then infiltrated with Spurr's resin through a resin:ethanol series of 1:1, 3:1, 100% Spurr's. After infiltration, the samples were cut into blocks of a width of 1 mm, placed in flat embedding molds, and polymerized at 70°C overnight. Ultrathin sections were cut using a diamond knife on a Reichert Ultracut S microtome (Leica Microsystems, Wetzlar, Germany), stained with 2% uranyl acetate, and visualized using a JEM-1230 TEM (Jeol, Tokyo, Japan). For each tissue sample, five randomly chosen fields were counted at 30000 $\times$  magnification and the diameter of 200 collagen fibrils was measured with an ocular micrometer. Results were the average of three independent experiments.

#### Atomic force microscopy

An atomic force microscope (AFM) (NanoScope IV; Veeco Digital Instruments, Santa Barbara, CA, USA) located at the Instrument Center of National Sun Yat-sen University (Kaohsiung, Taiwan, ROC) was utilized to scan the topography of the AM samples. All measurements were made in tapping mode with a silicon cantilever at room temperature. AFM images were recorded with a scan size of 50 nm  $\times$  50 nm. Five measurements were done on different surface sites to calculate the root mean square roughness (Rq) for each sample. Results were averaged on three independent runs.

#### In vitro degradation tests

To measure the extent of degradation, each test AM (1  $\times$  1 cm<sup>2</sup>) was first dried to constant weight ( $W_i$ ) in vacuo and was immersed in 1 ml of BSS containing 12  $\mu$ g collagenase at 37°C with reciprocal shaking (50 rpm) in a thermostatically controlled water bath. After 3 days, the membrane samples were taken out and washed with deionized water. The degraded samples were further dried in vacuo and weighed to determine the dry weight ( $W_d$ ). The percentage of weight remaining (%) was calculated as  $(W_d/W_i) \times 100$ . Results were the average of four independent measurements.

#### In vitro biocompatibility studies

In this study, HCE-2 cells, a human corneal epithelial cell line (ATCC No. CRL-11135), were purchased from the American Type Culture Collection (Manassas, VA, USA). The cells were

seeded on tissue culture plastics precoated with FNC Coating Mix, and maintained in regular growth medium containing KSFM, 0.05 mg/ml bovine pituitary extract, 5 ng/ml epidermal growth factor, 500 ng/ml hydrocortisone, and 0.005 mg/ml insulin. Cultures were incubated in a humidified atmosphere of 5% CO<sub>2</sub> at 37°C. The medium was changed twice a week. Cells were subcultured by trypsinization at a split ratio of 1:3.

A single extract of the test article was prepared using regular growth medium. The extracts were obtained by incubation of the sterilized AM materials with culture medium at 37°C for 24 h with an extraction ratio of 0.2 g/ml. Each test extract was then placed onto HCE-2 cell cultures with a seeding density of  $5 \times 10^4$  cells/well. After a 3-day incubation at 37°C in the presence of 5% CO<sub>2</sub>, the qualitative and quantitative assays were performed to examine the cellular responses to photo-cross-linked AM. The cells in regular growth medium without contacting material samples served as control groups.

Cell morphology was observed by phase-contrast microscopy (Nikon, Melville, NY, USA). Furthermore, cell viability was estimated using the CellTiter 96 Aqueous Non-Radioactive Cell Proliferation MTS Assay (Promega, Madison, WI, USA), in which MTS tetrazolium compound is bio-reduced by cells to form a water-soluble colored formazan.<sup>20</sup> The amount of colored product is proportional to the number of metabolically active cells. 100  $\mu$ l of the combined MTS/PMS (20:1) reagent was added to each well of the 24-well plate, and incubated for 3 h at 37°C in a CO<sub>2</sub> incubator. The data of absorbance readings at 490 nm were measured using the Multiskan Spectrum Microplate Spectrophotometer (ThermoLabsystems, Vantaa, Finland). All experiments were performed in quadruplicate, and the results were expressed as relative MTS activity when compared to control groups.

#### Anti-inflammatory activity studies

HCE-2 cells ( $5 \times 10^4$  cells/well) were seeded in 24-well plates containing regular growth medium and incubated overnight. For LPS stimulation, the medium was replaced with the fresh medium containing 1  $\mu$ g/ml, because high dosages of LPS ( $> 1 \mu$ g/ml) caused cell death and low dosages ( $< 0.01 \mu$ g/ml) showed little stimulation of cells.<sup>21</sup> Using cell culture inserts (Falcon 3095, Becton Dickinson Labware, Franklin Lakes, NJ, USA), each well of a 24-well plate was divided into two compartments. A sterilized membrane sample was placed into the inner well of the double-chamber system to examine the LPS-stimulated cultures after exposure to physically cross-linked AM materials. Unstimulated and LPS-stimulated HCE-2 cells without contacting the test samples served as the negative control (NC) and positive control (PC) groups, respectively.

After 3 days of incubation, the release of interleukin-6 (IL-6) from cultivated cells into the conditioned medium was detected by the Quantikine enzyme-linked immunosorbent assay (ELISA) kit (R&D Systems, Minneapolis, MN, USA) specific for human IL-6. Aliquots of the supernatant from each well were collected, and cytokine bioassays were performed according to the manufacturer's instructions. Photometric readings at 450 nm were measured using the Multiskan Spectrum Microplate Spectrophotometer (ThermoLabsystems). Results were expressed as pg/ml. All experiments were conducted in quadruplicate.



### Stemness gene and protein expression analyses

The rabbit corneoscleral rims were used to culture LECs. To disperse the cells, the corneoscleral rims were treated with dispase II at 37°C, followed by incubation with trypsin-EDTA solution. The cultures were maintained with supplemental hormonal epithelial medium (SHEM), which was made of an equal volume of HEPES-buffered DMEM containing bicarbonate and Ham's F-12, 0.5% DMSO, 2 ng/ml mouse epidermal growth factor, 5 µg/ml insulin, 5 µg/ml transferrin, 5 ng/ml selenium, 0.5 µg/ml hydrocortisone, 30 ng/ml cholera toxin A subunit, 5% FBS, 50 µg/ml gentamicin, and 1.25 µg/ml amphotericin B.

Rabbit LECs ( $5 \times 10^4$  cells/well) were seeded into 24-well TCPS plates (control groups) and various sterilized AM materials, and incubated in SHEM at 37°C for 5 days. Total RNA was isolated from cells with TRIzol reagent according to the manufacturer's procedure. Reverse transcription of the extracted RNA (1 µg) was performed using ImProm-II (Promega) and Oligo(dT)<sub>15</sub> primers (Promega). The primers used to amplify the rabbit ABCG2 cDNA were 5'-GAGAGCTGGGTCTGGAAAAAGT-3' (sense) and 5'-ATTCTTTTCAGGAGCAGAAGGA-3' (antisense). The sequences of the primer pair used to amplify the internal control cDNA, GAPDH, were 5'-TTGCCCTCAATGACCACTTG-3' (sense) and 5'-TTACTCCTTGAGGCCATGTG-3' (antisense). Quantitative real-time reverse transcription polymerase chain reaction (RT-PCR) was performed on a Light-Cycler instrument (Roche Diagnostics) according to the manufacturer's instructions with FastStart DNA Master SYBR Green I reagent (Roche Diagnostics). Each sample was determined in quadruplicate, and the gene expression results were normalized to the level of GAPDH mRNA.

The cells from each group were lysed in 1% NP-40 lysis buffer containing 1 mM EDTA, 1 mM ethylene glycol tetraacetic acid, 5 µg/ml antipain, 5 µg/ml pepstatin A, 1 mM phenylmethylsulfonyl fluoride, and 5 µg/ml aprotinin to prepare protein extracts for Western blot analyses. Protein concentrations were determined by protein assay (Bio-Rad, Hercules, CA, USA) and 50 µg of protein per lane was separated by electrophoresis under reducing conditions in 10% polyacrylamide gel with sodium dodecyl sulfate (SDS-PAGE). For Western blotting, SDS-PAGE gels were transferred to poly(vinylidene difluoride) membranes that were blocked with 5% nonfat milk in tris-HCl-buffered saline containing 0.1% Tween-20 (TTBS) for 1 h at room temperature. The membranes were then incubated with anti-ABCG2 (1:1000; Santa Cruz Biotechnology, Santa Cruz, CA, USA) primary antibodies with 5% nonfat milk in TTBS overnight at 4°C with gentle rocking. Next, blots were washed for three times with 0.1% TTBS solution and incubated with secondary antibodies conjugated to horseradish peroxidase (1:5000; Chemicon International, Temecula, CA, USA) with 5% nonfat milk in TTBS for 1 h at room temperature. The SuperSignal West Pico chemiluminescent substrate (Pierce, Rockford, IL, USA) was used for detecting a secondary antibody on imaging films (Biomax MS, Eastman Kodak, Rochester, NY, USA). Anti-alpha-tubulin (1:2000; Abcam, Cambridge, MA, USA) was used as loading controls. ABCG2 protein bands were analyzed by densitometry using ImageJ software. Results were the average of four independent measurements.

### Statistics

Results were expressed as mean  $\pm$  standard deviation. Comparative studies of means were performed using one-way analysis of variance (ANOVA). Significance was accepted with  $p < 0.05$ .

## Results and discussion

### Preparation of photo-cross-linked amniotic membranes

Human AM derives from the innermost layer of the placental membrane and consists of a thick basement membrane and an avascular stromal matrix.<sup>1</sup> In terms of AM specimen collection and processing, the sources of biological variations may impact the material performance in potential application as a tissue engineering scaffold. To avoid position effects, the tissue samples are cut with a scalpel blade approximately 2 cm from the placental disc since there is regional variability of donor AM.<sup>22</sup> However, the batch-to-batch variations do exist in biological material itself. Furthermore, given that the fact that the biological tissue is not an artificial material, its thickness cannot be adequately controlled during AM preparation. In this study, the in vitro degradability is calculated based on normalization of initial weight values of samples. To further obtain reliable characterization results, the AM with an average thickness of 100 µm is used for the development of photo-cross-linked scaffold material for LEC cultivation.

For AM photo-cross-linking, the biological tissues were treated with riboflavin and UV light. As reported in the literature, the mechanisms of corneal cross-linking in response to treatment with topical riboflavin and UV radiation may involve the production of singlet oxygen and subsequent formation of physical cross-links in the tissue collagen.<sup>23</sup> Riboflavin-catalyzed photosensitization, photooxidation, and photopolymerization are believed to play direct roles in the photo-cross-linking of AM collagen molecules. Recently, Mu et al. have shown that the incubation of engineered 3D hydrogel vascular network in ribose solution improves the mechanical integrity and hydrolysis resistance of the collagen fibrils.<sup>24</sup> In comparison with riboflavin (i.e., a photosensitizer), ribose is a reducing sugar that can cross-link collagen by reacting with amine groups. Although several cross-linking strategies are currently available to improve the stability of ocular tissue collagen, the physical and chemical methods are different in nature.<sup>25</sup> The technique of riboflavin treatment and UV irradiation can be successfully employed to induce physical cross-links in keratoconus corneas. By contrast, for chemical modification of biological tissue samples, the treatment of ribose leads to glycation-induced cross-linking, but is relatively ineffective in strengthening bonding.

### Cross-linking density measurements

Although UV-activated riboflavin is commonly used in the treatment of corneal diseases, the application of this photo-cross-linking technique for the modification of AM collagen has not been previously reported in the literature. Here, we studied the effect of photoinitiator concentration on the preparation of physically cross-linked biological tissue materials. Fig. 1 shows the cross-linking density of AM as a function of riboflavin concentration. A higher photo-cross-linking density represents a

greater mechanical stability.<sup>26</sup> In the AM-0.1, AM-1, and AM-10 groups, the number of cross-links per unit mass of tissue collagen matrix determined by mechanical tests was  $2.26 \pm 0.10$ ,  $6.18 \pm 0.22$ , and  $8.02 \pm 0.19$  cross-links/mol. wt  $10^5$ , respectively, which indicates that the cross-linking density is significantly increased with an increase in photoinitiator concentration ( $p < 0.05$ ). Our previous report has shown that the cross-linking density of synthesized 2-hydroxyethyl methacrylate and acrylic acid copolymers strongly depends on the 2,2-diethoxyacetophenone concentration in the UV photoinitiation system of radical polymerization.<sup>18</sup> The present data are compatible with these earlier observations. It is also noteworthy that the increment of the number of cross-links per unit mass of AM is not proportional to the photoinitiator concentration. This implies that the amount of UV-activated riboflavin may be associated with a significantly different extent of change in the cross-linked structure of AM collagen. According to related experiences of chemical cross-linking of solid membrane samples in liquid cross-linking agents, the ability of cross-linkers to penetrate into the interior of the AM is very critical to determine the intermolecular collision frequency and hence cross-linking efficiency.<sup>8,10</sup> One potential explanation for the results of this study is that when treated with relatively high concentration (i.e., 10 mg/ml) of riboflavin, the biological tissue material does not completely contain the photoinitiator due to the limited penetration.

#### Water content measurements

Collagen is known to have a high water absorption and retention capacity. Since the UV irradiation-mediated change in the cross-linked structure of AM samples is noted in this article, the water content of modified collagenous tissue materials may be affected by photoinitiator concentration. Therefore, the physically cross-linked AM was studied to determine its water absorbing capacity. Fig. 2 shows the equilibrium water content of AM as a function of riboflavin concentration. After incubation in deionized water at 37°C for 6 h, the biological tissues from AM-0 groups had an equilibrium water content of  $88.6 \pm 0.9\%$ , which was significantly higher than those of the photo-cross-linked counterparts ( $p < 0.05$ ). The result indicates that the treatment of AM with riboflavin and UV light can enhance the hydrophobicity of the matrix. Furthermore, the water absorbing capacity significantly decreased with increasing photoinitiator concentration from 0.1 to 10 mg/ml. It has been reported that a low level of degree of hydration of collagen fibers is attributed to the cross-linker-mediated structural alteration in biological tissues.<sup>9</sup> The introduction of higher amounts of cross-links in the carbodiimide-treated AM brings the collagen molecules closer together, thereby causing a greater extent of dehydration of fibers. For the first time, our data demonstrate that the cross-linked structure of UV-irradiated AM materials with different cross-linking densities may play an important role in regulating the equilibrium water content of tissue collagen. Given that the water content is a useful parameter that is central to the understanding of cross-linking degree of AM collagen, the water absorbing capacity of the modified tissue materials is evaluated for varying photo-cross-linking conditions. These measurements support the results gained by cross-linking density measurements (Fig. 1).

#### Transmission electron microscopy

As demonstrated by the aforementioned findings, the UV irradiation is a technique capable of inducing formation of new cross-links in the tissue collagen matrix, which helps to construct the architectural framework of the AM. To investigate whether the photo-cross-linking can mediate nanostructural changes in the AM materials, the TEM observations are performed. Fig. 3 shows the ultrastructure of AM as a function of riboflavin concentration. In the AM-0 groups, the biological tissue without photo-cross-linking is composed of small diameter (approximately 60 nm) collagen fibrils. However, after the treatment of AM with riboflavin and UV light, large size fibrillar bundles were noted. With increasing photoinitiator concentration from 0.1 to 10 mg/ml, the aggregation of collagen fibrils was significantly augmented. There were statistically significant differences in the fiber diameter between the AM-0.1 ( $135 \pm 28$  nm), AM-1 ( $292 \pm 26$  nm), and AM-10 ( $390 \pm 41$  nm) groups ( $p < 0.05$ ). These findings suggest that the ultrastructure of UV-irradiated collagenous tissue materials is largely affected by photoinitiator concentration. We also provide clear evidence of a relationship between collagen nanofiber size and the number of cross-links generated during AM photo-cross-linking.

#### Atomic force microscopy

Our group has recently investigated the effects of carbodiimide cross-linking on the AM matrix alignment, shape, and texture.<sup>9</sup> The topographical feature of the collagenous tissue materials is found to be associated with the molecular fibrillar structure. Here, we examined the nanoscale surface characteristics of the photo-cross-linked AM substrates. Fig. 4 shows the tapping mode AFM height images of various AM samples. In the AM-0 groups, the biological tissues contained randomly aligned fibrils. After photo-cross-linking of the membranes, the ordered organization of collagen fibrils was noted. In addition, with increasing photoinitiator concentration from 0.1 to 10 mg/ml, the UV-irradiated biological tissues exhibited rougher surface topography. The samples with higher number of cross-links per unit mass of AM had even some ridges. The cross-link-induced aggregation of tropocollagen molecules also causes the change in surface roughness. There were statistically significant differences in the Rq between the AM-0 ( $5.6 \pm 0.5$  nm), AM-0.1 ( $8.2 \pm 0.9$  nm), AM-1 ( $13.0 \pm 1.1$  nm), and AM-10 ( $21.7 \pm 2.8$  nm) groups ( $p < 0.05$ ). It is known that during fixation, the tissue shrinks in size, thereby affecting the material structure and surface morphology. Sung et al. have reported that the shrinkage of chemically cross-linked porcine pericardium is attributed to the contraction of the tropocollagen molecules and collagen networks.<sup>27</sup> This may explain that a large amount of cross-links present in the biopolymer structure is involved in the nanotopographical roughness of UV-irradiated AM.

#### In vitro degradation tests

More recently, we have shown that the increase in chemical cross-linker concentration from 0.001 to 0.03 mmol glutaraldehyde per mg AM may lead to significant enhancement of resistance to collagenolytic degradation, indicating the role of cross-linking density of AM in the degradation behavior.<sup>19</sup> In the present study, the AM was treated with varying concentrations of

riboflavin and UV light to decrease the *in vitro* enzymatic degradability of tissue collagen. In order to further understand the matrix stability due to the variation of cross-linked structure of photo-cross-linked AM, the biological tissues were incubated in BSS containing collagenase. Fig. 5 shows the residual mass percentage of various AM samples after 3 days of degradation. In the AM-0 groups, the enzymatic digestion of biological tissue without photo-cross-linking was responsible for approximately 65% of weight loss. The remaining weight in the AM-0.1, AM-1, and AM-10 groups was  $41.9 \pm 1.0$ ,  $55.2 \pm 1.3$ , and  $64.7 \pm 2.8\%$ , respectively. The values showed significant differences between these three groups ( $p < 0.05$ ), which suggested that the photoinitiator concentration had a certain influence on the biological stability of physically cross-linked AM collagen.

### In vitro biocompatibility studies

Fig. 6 shows representative phase-contrast micrographs of HCE-2 cell cultures after incubation for 3 days at 37°C with extract medium conditioned with various AM samples. Control cultures displayed a cobblestone-like morphology typical of normal corneal epithelial cells. In the AM-0 groups, the HCE-2 cell cultures appeared healthy, indicating that the test extracts prepared from non-cross-linked biological tissue materials do not cause human corneal epithelial cell damage. The cultures in the AM-0.1, AM-1, and AM-10 groups also showed a similar cell growth pattern to that seen in the control groups. Our findings suggest that corneal epithelial cell morphology is not altered after exposure to the test articles. Irrespective of the photoinitiator concentration, the photo-cross-linked AM samples have good compatibility with HCE-2 cell growth.

Fig. 7 further shows the results of proliferation assay of human corneal epithelial cell cultures incubated with extract medium conditioned with various AM samples for 3 days. The mitochondrial dehydrogenase activity (MTS activity) of cells grown in the absence of test materials (i.e., control groups) was set to 100%. In the AM-0 groups, the measured activity level was  $99.0 \pm 0.9\%$ , which was not significantly different compared with AM-0.1 ( $99.2 \pm 1.3\%$ ), AM-1 ( $98.1 \pm 2.1\%$ ), and AM-10 ( $96.9 \pm 1.5\%$ ) groups ( $p > 0.05$ ). The results indicate that the HCE-2 cells remain metabolically active even after they are exposed to the test articles for 3 days, implying no cytotoxicity of these photo-cross-linked AM matrices.

The AM is a valuable biological material that exhibits good biocompatibility. We have previously investigated the ocular tissue responses to AM by using the anterior chamber of a rabbit eye model and concluded that the biological tissue implants do not induce any foreign body reaction during the follow-up period of three years.<sup>28</sup> In order to improve the stability of tissue collagen, the AM has been modified with a commonly used homobifunctional cross-linker such as glutaraldehyde.<sup>6,29</sup> However, our recent study has revealed that when the treatment duration is increased from 6 to 24 h, the cytotoxicity of glutaraldehyde cross-linked AM increases dramatically.<sup>10</sup> In addition, the relationship between cross-linker concentration and cytocompatibility of glutaraldehyde-treated AM has been explored in our laboratory.<sup>19</sup> It is noted that while the biological tissues with relatively high cross-linking densities display poor compatibility with HCE-2 cultures, the AM samples cross-linked with lower concentrations (i.e.,  $< 0.03$  mmol glutaraldehyde per

mg AM) do not significantly affect the proliferative capacity of the cells. Therefore, it is necessary to evaluate the safety of photo-cross-linked AM as a new carrier before application to the cultivation of LECs. The findings of the present work suggest that the AM treated with riboflavin and UV light is fully biocompatible towards corneal epithelial cells due to the absence of exogenous cross-linker molecules in the proteinaceous matrices following cross-linking reaction. In addition, given that the cells survive well after exposure to the AM materials prepared from different riboflavin concentrations, these physically cross-linked biological tissues have great potential for further development of corneal epithelial cell culture platform.

### Anti-inflammatory activity studies

In our laboratory, the AM is found to be involved in the enhanced generation of anti-angiogenic/anti-inflammatory factors in human limbo-corneal epithelial cells, thereby leading to rapid restoration of corneal avascularity after cultivated epithelial stem cell transplantation.<sup>30</sup> As one of the major cytokine-triggering mediators of inflammatory reactions, IL-6 appears to be especially relevant in corneal grafting.<sup>31</sup> Therefore, the anti-inflammatory properties of photo-cross-linked AM tissues were studied by ELISA to analyze the expression of secreted pro-inflammatory cytokine such as IL-6. Fig. 8 shows the IL-6 levels in the media after 3 days of incubation of corneal epithelial cell cultures with various AM samples. In the NC groups, the measured concentration of IL-6 was  $38.8 \pm 6.5$  pg/ml, which was significantly lower than those of the PC ( $1490.4 \pm 31.7$  pg/ml) groups ( $p < 0.05$ ). It indicates that LPS can stimulate HCE-2 cells to secrete the pro-inflammatory cytokine. On the other hand, there was no statistically significant difference in the IL-6 level between the AM-0 ( $391.6 \pm 25.9$  pg/ml), AM-0.1 ( $420.7 \pm 33.0$  pg/ml), AM-1 ( $401.1 \pm 34.9$  pg/ml), and AM-10 ( $440.6 \pm 37.2$  pg/ml) groups ( $p > 0.05$ ). The findings of the present work suggest that the AM samples treated with riboflavin and UV light retain anti-inflammatory activities similar to their non-cross-linked counterparts. In contrast, the AM cross-linked with glutaraldehyde for 24 h can significantly upregulate the gene expression of interleukin-6 and the production of tumor necrosis factor- $\alpha$  in HCE-2 cultures, indicating that the chemical cross-linker may cause the cells to release cytokine-triggering mediators of inflammatory reactions.<sup>10</sup> Furthermore, although the glutaraldehyde cross-linked AM materials still have some anti-inflammatory activities, the increase in cross-linking density leads to the upregulation of IL-6 cytokine levels in LPS-stimulated cells.<sup>19</sup> It is also noted that the photoinitiator concentration seems not to be a governing factor for the modulation of anti-inflammatory properties of physically cross-linked biological materials. One potential explanation for the results is that the absence of exogenous cross-linker molecules in the AM matrices following photo-cross-linking reaction does not impair the protein function and consequent anti-inflammatory action.

### Stemness gene and protein expression analyses

In the research field of ocular surface reconstruction, the regulation of limbal stem cell niche is of great importance to preserve the progenitors of LECs. Human AM tissue has been investigated as a limbal epithelial stem cell niche since this



biological material is able to maintain the undifferentiated precursor cell phenotype.<sup>32-36</sup> We have demonstrated that when compared to their non-cross-linked counterparts, the AM materials cross-linked with carbodiimide<sup>9</sup> or glutaraldehyde<sup>10</sup> significantly promote the expressions of stem cell markers such as ABCG2 and p63. In addition, the extent of cross-linking of biological tissues has a profound influence on the maintenance of stemness (i.e., undifferentiated state) in LEC cultures. To investigate whether the photo-cross-linked AM can be used as a LEC carrier, the quantitative real-time RT-PCR assay is performed. Fig. 9 shows the ABCG2 gene expression of rabbit LECs after growth on various AM samples for 5 days. In the control groups (i.e., absence of AM materials), the mRNA level was defined as 100%. In the AM-0 groups, the ABCG2 gene expression was  $138.5 \pm 13.0\%$ . It was significantly lower than those of the AM-0.1 ( $169.0 \pm 17.7\%$ ), AM-1 ( $286.5 \pm 10.8\%$ ), and AM-10 ( $361.4 \pm 25.2\%$ ) groups ( $p < 0.05$ ), indicating that the AM samples treated with riboflavin and UV light may enhance the stemness gene expression levels.

In order to examine whether the alterations in gene expressions are correlated to altered protein levels, Western blotting is also performed in this study. Fig. 10 shows the results of ABCG2 protein expression detection in rabbit LECs after 5 days of cultivation on various AM samples. Western blot analysis with an antibody for ABCG2 demonstrated a 70-kDa band in these cell lysates. Similar protein expression patterns were observed between the control, AM-0, and AM-0.1 groups. However, the cultures from the AM-1 and AM-10 groups showed more intense protein bands. The differences in protein signal intensities were further analyzed by densitometry using ImageJ software. As shown in Fig. 11, the y-axis reflects arbitrary density units. When compared to their non-cross-linked counterparts, the photo-cross-linked AM substrates significantly promote the protein expression of ABCG2 in LECs ( $p < 0.05$ ). Furthermore, among the samples treated with varying concentrations of photoinitiator, 10 mg/ml of riboflavin showed the highest expression levels of ABCG2. The findings of the stemness protein expression support the data from the gene expression assays and suggest that the cross-linked structure of tissue collagen may affect the cell stemness during ex vivo limbal epithelial expansion on AM matrices. It is known that during the growth on the culture surfaces in vitro, the stem cells can sense the nanotopographical features of the substrate matrix.<sup>37</sup> Therefore, the surface roughness of photo-cross-linked AM is considered to be one of the major factors regulating cell behaviors. A study from Marletta et al. has reported that with increasing surface nanoroughness of ion-induced chemically structured poly- $\epsilon$ -caprolactone films, the cultivated human marrow stromal cells seem unfavorable for osteogenic differentiation.<sup>38</sup> Our group has recently investigated the effects of surface roughness of hyaluronic acid coatings on the fabrication of corneal keratocyte spheroid and its self-renewal potential.<sup>39</sup> The expression levels of nestin (i.e., a neural progenitor cell-specific marker) were higher in larger-sized spheroids cultured on the surfaces with a rough topography. In accordance with these earlier observations, we demonstrate that the nanotopographical roughness of photo-cross-linked AM dictates the stemness expressions at mRNA and protein levels. On the other hand, Seidlits et al. have shown that when compared

to their counterparts with lower moduli, the stiffer hyaluronic acid hydrogels are unable to promote the differentiation of encapsulated ventral mesencephalic neural progenitors.<sup>40</sup> Given that the cell differentiation ability strongly depends on matrix stiffness, the mechanical properties of photo-cross-linked AM correlated with the photoinitiator concentration may also contribute to the maintenance of stemness in LEC cultures. In the future, taking the advantages of photo-cross-linking-mediated surface nanotopographical features, the behaviors of LECs cultured on the UV-irradiated biological tissues can be adequately controlled through the design of the stable AM scaffolds with tunable cross-linking densities.

## Conclusions

In this work, the physically cross-linked AM materials were successfully prepared by the photo-cross-linking method with various amounts of UV-activated riboflavin. The number of cross-links per unit mass of tissue collagen matrix was significantly increased with an increase in photoinitiator concentration from 0.1 to 10 mg/ml. In addition, the equilibrium water content and mechanical and biological stabilities of AM collagen were found to be associated with the cross-linked structure of UV-irradiated biological tissue samples. The number of cross-links generated during AM photo-cross-linking could regulate the ultrastructure of nanofibrous collagen scaffolds. The AM substrates with higher cross-linking degrees exhibited rougher topographies. Irrespective of the riboflavin concentration, the photo-cross-linked AM was fully biocompatible towards corneal epithelial cells and retained anti-inflammatory activities, probably due to the absence of exogenous cross-linker molecules in the proteinaceous matrices following cross-linking reaction. In vitro cell culture studies showed that the LECs grown on the AM substrates with different cross-linking densities and surface roughnesses had varying levels of enhanced stemness. For the first time, here we demonstrate that the riboflavin concentration may play an important role in the modulation of properties of photo-cross-linked AM as a new LEC carrier.

## Acknowledgements

This work was supported by grant NSC100-2628-E-182-004-MY3 from the National Science Council of Republic of China. The author is grateful to Dr. David Hui-Kang Ma (Department of Ophthalmology, Chang Gung Memorial Hospital) and Miss Hsiao-Yun Cheng (Molecular Medicine Research Center, Chang Gung University) for technical assistance.

## Notes and references

- <sup>a</sup> Institute of Biochemical and Biomedical Engineering, Chang Gung University, Taoyuan 33302, Taiwan, ROC. E-mail: jylai@mail.cgu.edu.tw; Fax: +886 3 2118668; Tel: +886 3 2118800 ext. 3598
- H. S. Dua, J. A. P. Gomes, A. J. King and V. S. Maharajan, *Surv. Ophthalmol.*, 2004, **49**, 51-77.
  - K. Iijima, Y. Igawa, T. Imamura, T. Moriizumi, T. Nikaido, I. Konishi and O. Nishizawa, *Tissue Eng.*, 2007, **13**, 513-524.
  - L. Yang, Y. Shirakata, S. Tokumaru, D. Xiuju, M. Tohyama, Y. Hanakawa, S. Hirakawa, K. Sayama and K. Hashimoto, *J. Dermatol. Sci.*, 2009, **56**, 188-195.



- 4 J. Y. Lai and G. H. Hsiue, *React. Funct. Polym.*, 2007, **67**, 1284-1291.
- 5 R. J. F. Tsai, L. M. Li and J. K. Chen, *N. Engl. J. Med.*, 2000, **343**, 86-93.
- 6 T. Fujisato, K. Tomihata, Y. Tabata, Y. Iwamoto, K. Burczak and Y. Ikada, *J. Biomater. Sci. Polym. Ed.*, 1999, **10**, 1171-1181.
- 7 H. H. Slansky and C. H. Dohlman, *Surv. Ophthalmol.*, 1970, **14**, 402-415.
- 8 D. H. K. Ma, J. Y. Lai, H. Y. Cheng, C. C. Tsai and L. K. Yeh, *Biomaterials*, 2010, **31**, 6647-6658.
- 9 J. Y. Lai, S. J. Lue, H. Y. Cheng and D. H. K. Ma, *J. Biomed. Nanotechnol.*, 2013, **9**, 2048-2062.
- 10 J. Y. Lai and D. H. K. Ma, *Int. J. Nanomed.*, 2013, **8**, 4157-4168.
- 11 P. L. Lu, J. Y. Lai, D. H. K. Ma and G. H. Hsiue, *J. Biomater. Sci. Polym. Ed.*, 2008, **19**, 1-18.
- 12 J. Y. Lai, Y. T. Li and T. P. Wang, *Int. J. Mol. Sci.*, 2010, **11**, 5256-5272.
- 13 J. Y. Lai and Y. T. Li, *Mater. Sci. Eng. C*, 2010, **30**, 677-685.
- 14 J. Y. Lai, *J. Mech. Med. Biol.*, 2011, **11**, 967-981.
- 15 C. Nishi, N. Nakajima and Y. Ikada, *J. Biomed. Mater. Res.*, 1995, **29**, 829-834.
- 16 H. Hashemi, M. A. Seyedian, M. Mirafab, A. Fotouhi and S. Asgari, *Ophthalmology*, 2013, **120**, 1515-1520.
- 17 J. Y. Lai, K. H. Chen and G. H. Hsiue, *Transplantation*, 2007, **84**, 1222-1232.
- 18 J. Y. Lai, T. P. Wang, Y. T. Li and I. H. Tu, *J. Mater. Chem.*, 2012, **22**, 1812-1823.
- 19 J. Y. Lai, *RSC Adv.*, 2014, **4**, 18871-18880.
- 20 J. Y. Lai and Y. T. Li, *Biomacromolecules*, 2010, **11**, 1387-1397.
- 21 D. H. Kim, M. T. Novak, J. Wilkins, M. Kim, A. Sawyer and W. M. Reichert, *Biomaterials*, 2007, **28**, 4231-4239.
- 22 S. P. Wilshaw, J. Kearney, J. Fisher and E. Ingham, *Tissue Eng. Part A*, 2008, **14**, 463-472.
- 23 A. S. McCall, S. Kraft, H. F. Edelhauser, G. W. Kidder, R. R. Lundquist, H. E. Bradshaw, Z. Dedeic, M. J. C. Dionne, E. M. Clement and G. W. Conrad, *Invest. Ophthalmol. Vis. Sci.*, 2010, **51**, 129-138.
- 24 X. Mu, W. Zheng, L. Xiao, W. Zhang and X. Jiang, *Lab Chip*, 2013, **13**, 1612-1618.
- 25 G. Wollensak and E. Spoerl, *J. Cataract. Refract. Surg.*, 2004, **30**, 689-695.
- 26 H. Tai, W. Wang, T. Vermonden, F. Heath, W. E. Hennink, C. Alexander, K. M. Shakesheff and S. M. Howdle, *Biomacromolecules*, 2009, **10**, 822-828.
- 27 H. W. Sung, W. H. Chang, C. Y. Ma and M. H. Lee, *J. Biomed. Mater. Res.*, 2003, **64A**, 427-438.
- 28 P. L. Lu, J. Y. Lai, Y. Tabata and G. H. Hsiue, *J. Biomed. Mater. Res.*, 2008, **86A**, 108-116.
- 29 E. Spoerl, G. Wollensak, F. Reber and L. Pillunat, *Ophthalmic Res.*, 2004, **36**, 71-77.
- 30 D. H. K. Ma, H. C. Chen, J. Y. Lai, C. C. Sun, S. F. Wang, K. K. Lin and J. K. Chen, *Ocul. Surf.*, 2009, **7**, 128-144.
- 31 R. Hoekzema, C. Verhagen, M. van Haren and A. Kijlstra, *Invest. Ophthalmol. Vis. Sci.*, 1992, **33**, 532-539.
- 32 M. Grueterich, E. M. Espana and S. C. G. Tseng, *Surv. Ophthalmol.*, 2003, **48**, 631-646.
- 33 R. M. Lavker, S. C. G. Tseng and T. T. Sun, *Exp. Eye Res.*, 2004, **78**, 433-446.
- 34 M. A. Stepp and J. D. Zieske, *Ocul. Surf.*, 2005, **3**, 15-26.
- 35 P. Ordonez and N. Di Girolamo, *Stem Cells*, 2012, **30**, 100-107.
- 36 D. H. K. Ma, J. Y. Lai, S. T. Yu, J. Y. Liu, U. Yang, H. C. Chen, L. K. Yeh, Y. J. Ho, G. Chang, S. F. Wang, J. K. Chen and K. K. Lin, *J. Cell. Physiol.*, 2012, **227**, 2030-2039.
- 37 M. J. Dalby, N. Gadegaard and R. O. C. Oreffo, *Nat. Mater.*, 2014, **13**, 558-569.
- 38 G. Marletta, G. Ciapetti, C. Satriano, F. Perut, M. Salerno and N. Baldini, *Biomaterials*, 2007, **28**, 1132-1140.
- 39 J. Y. Lai and I. H. Tu, *Acta Biomater.*, 2012, **8**, 1068-1079.
- 40 S. K. Seidlits, Z. Z. Khaing, R. R. Petersen, J. D. Nickels, J. E. Vanscoy, J. B. Shear and C. E. Schmidt, *Biomaterials*, 2010, **31**, 3930-3940.

## Figure Captions

**Fig. 1** Number of cross-links per unit mass of AM as a function of riboflavin concentration. Values are mean  $\pm$  standard deviation ( $n = 4$ ). \* $p < 0.05$  vs all groups.

**Fig. 2** Equilibrium water content of various AM samples. Values are mean  $\pm$  standard deviation ( $n = 4$ ). \* $p < 0.05$  vs all groups.

**Fig. 3** Representative transmission electron microscopic images of various AM samples. (a) AM-0, (b) AM-0.1, (c) AM-1, and (d) AM-10 groups. Scale bars: 200 nm. Theoretically, there is no new collagen molecule and fiber produced by photo-cross-linking, indicating no increase in the concentration of total collagen fibers. However, with increasing photoinitiator concentration from 0.1 to 10 mg/ml, the total collagen fibers in TEM images appear to be increasing, mainly due to that numerous collagen fibrils aggregate and combine to form larger-sized fibers within the regions of the image frames.

**Fig. 4** Representative atomic force microscopic images of various AM samples. (a) AM-0, (b) AM-0.1, (c) AM-1, and (d) AM-10 groups.

**Fig. 5** Weight remaining of various AM samples after incubation at 37°C for 3 days in BSS containing collagenase. Values are mean  $\pm$  standard deviation ( $n = 4$ ). \* $p < 0.05$  vs all groups.

**Fig. 6** Phase-contrast micrographs of HCE-2 cell cultures. The pattern of cell growth in (a) controls (without materials) after incubation for 3 days at 37°C with extract medium conditioned with various AM samples (b) AM-0, (c) AM-0.1, (d) AM-1, and (e) AM-10. Scale bars: 50  $\mu$ m.

**Fig. 7** Cell proliferation assay of HCE-2 cell cultures incubated with extract medium conditioned with various AM samples for 3 days. Results are expressed as percentage of controls (MTS activity of cells cultured in the absence of materials). Values are mean  $\pm$  standard deviation ( $n = 4$ ).

**Fig. 8** Level of IL-6 released from HCE-2 cell cultures after incubation with various AM samples for 3 days. Unstimulated and LPS-stimulated cells without contacting the test materials were the NC and PC groups, respectively. Values are mean  $\pm$  standard deviation ( $n = 4$ ). \* $p < 0.05$  vs all groups; # $p < 0.05$  vs NC and PC groups.

**Fig. 9** Gene expression level of ABCG2 in rabbit LECs grown on various AM samples for 5 days, measured by real-time RT-PCR. Normalization was done by using GAPDH. Data in the experimental groups are percentages relative to that of control groups (cells cultured on TCPS in the absence of AM materials). Values are mean  $\pm$  standard deviation ( $n = 4$ ). \* $p < 0.05$  vs all groups.

**Fig. 10** Western blot analysis of ABCG2 expression in rabbit LECs grown on various AM samples for 5 days. Lane 1: control (cells cultured on TCPS in the absence of AM materials), Lane 2: AM-0, Lane 3: AM-0.1, Lane 4: AM-1, and Lane 5: AM-10 groups.

**Fig. 11** Western blot analysis-based ABCG2 expression in rabbit LECs grown on various AM samples for 5 days. The intensity of ABCG2

relative to total protein measured by densitometry using ImageJ software.  
Values are mean  $\pm$  standard deviation ( $n = 4$ ). \* $p < 0.05$  vs all groups.

Fig. 1

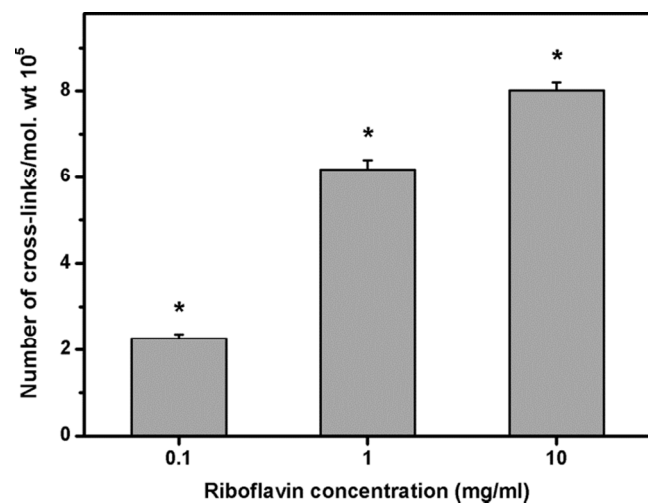


Fig. 2

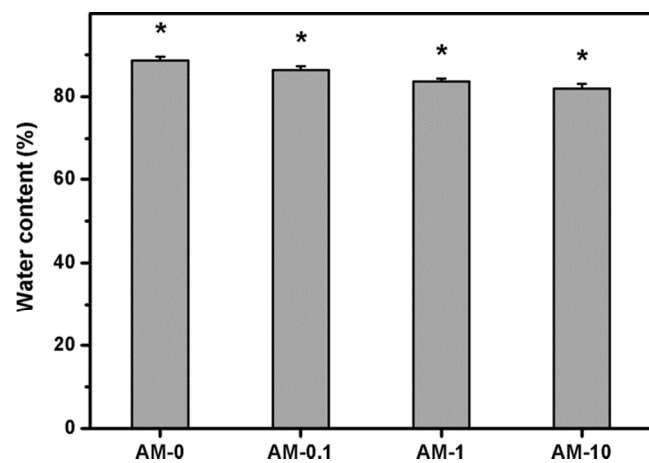


Fig. 3

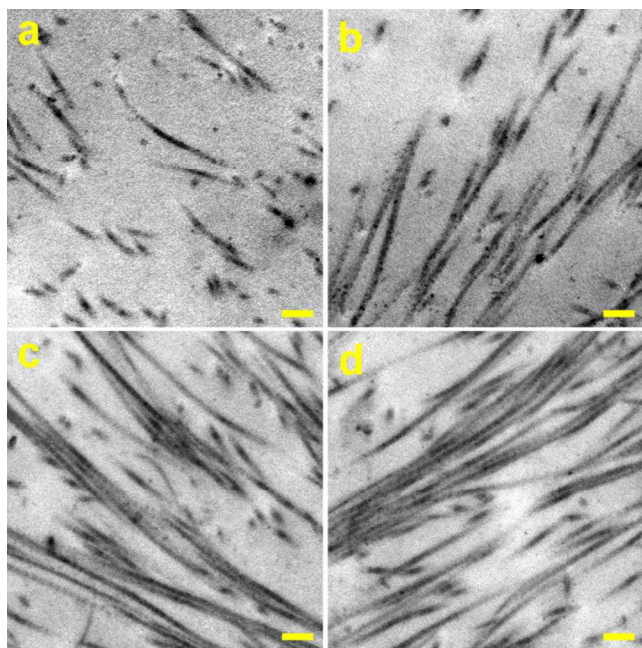




Fig. 4

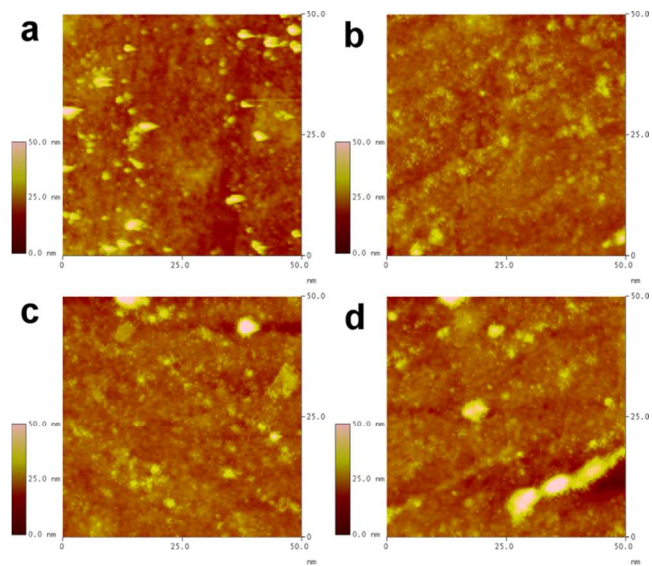


Fig. 5

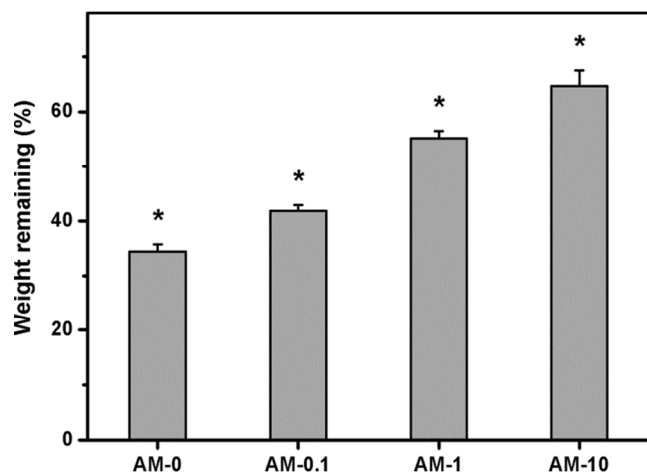


Fig. 6

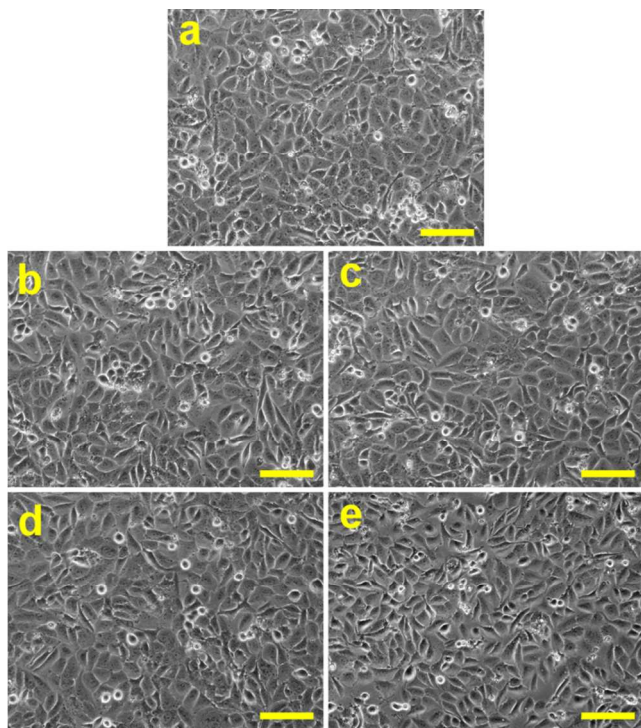


Fig. 7

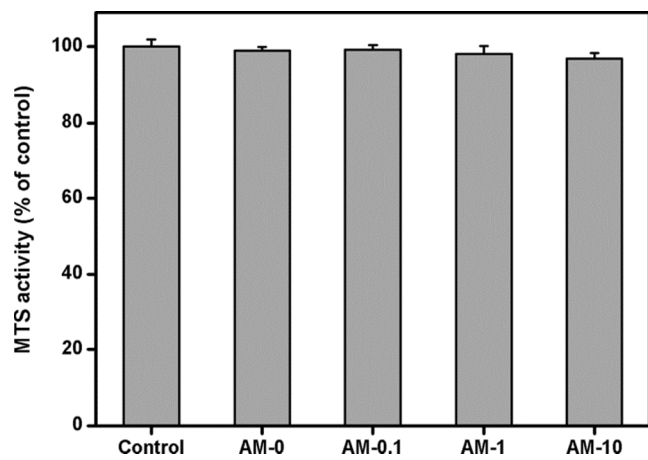




Fig. 8

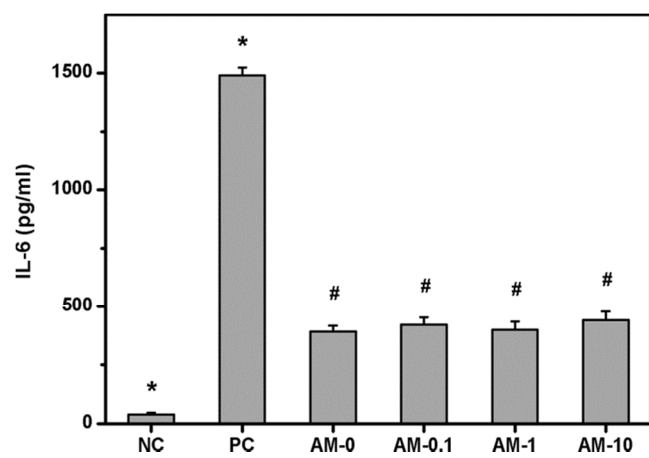


Fig. 9

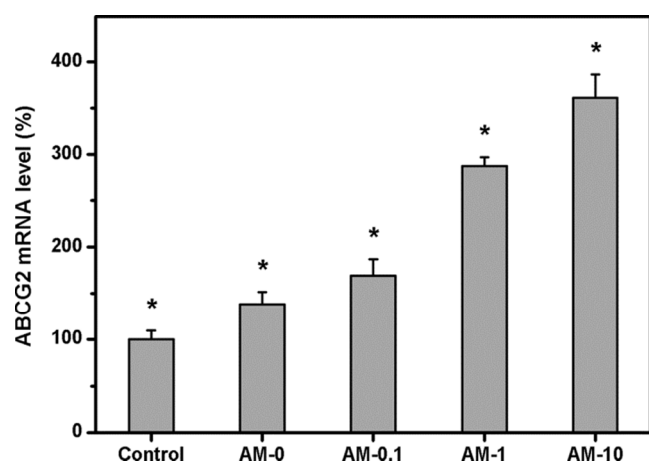


Fig. 10

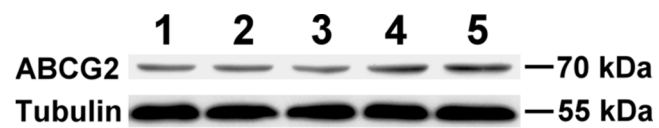
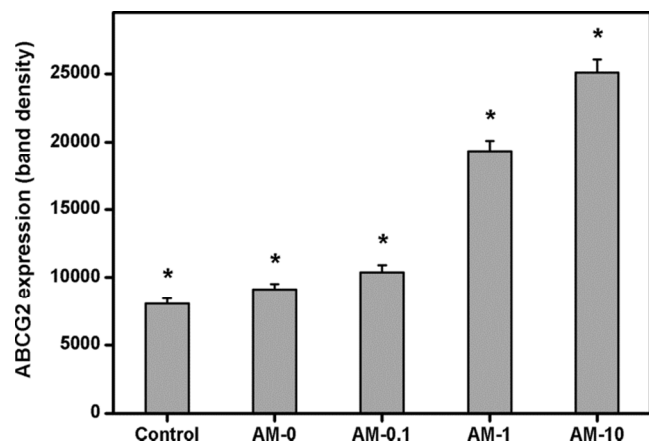


Fig. 11







Riboflavin concentration is critical to tailor the cross-linking degree of the collagen network and thus the nanostructure of photo-cross-linked amniotic membrane for cultivation of limbal stem cells.

### Role of AM Nanotopography in LEC Stemness

